in the spectra of either the nonspinning sample or of an unfilled, nonvulcanized, otherwise comparable, *cis*-polyisoprene. This line appeared in every spectrum obtained at the magic angle and its position and intensity were reproducible. Qualitative indications of its spin–lattice relaxation time suggested a longer value than for normal main-chain methylene carbons, but shorter values than for normal methyl carbons in *cis*-polyisoprene. Several kinds of lines arising from structural and steric defects in the polymer chain can occur in this region,[2] so an unambiguous assignment is not possible at this time. One possibility is that the line arises from methylene carbons which have been removed from the main chain during vulcanization, remain bonded to carbons still in the chain, but are now also covalently bonded to sulfur and so form part of the cross-linking network. On the other hand, the line may simply arise from carbons in independent chain fragments, either formed during the milling or vulcanization processes, or part of the oil additives usually found in rubber formulations.

Magic-angle spinning experiments on solid rubbers have been reported before. In fact, the proton nmr line of a cross-linked silicone rubber has been successfully narrowed in both magic-angle spinning[14] and multiple-pulse experiments.[15]

(14) M. Cohn, A. Kowalsky, J. Leigh, and S. Maricic, "Magnetic Resonance in Biological Systems," Pergamon Press, Elmsford, N. Y., 1967, p 45.

(15) L. M. Huber, unpublished results, as cited in ref 3a.

These earlier results were interpreted in terms of the net slow motion of the chains, generating a distribution of interchain interactions which occurred almost entirely at low frequencies. In the carbon-black-filled polyisoprene system, low-frequency interactions probably arise from filler–chain entanglements. That is, the filler excludes the bulk polymer from some spatial orientations resulting in low-frequency dipolar interactions which are not averaged to zero in a time $T_2$. The nmr lines are therefore subject to incomplete motional narrowing. Since the $^{13}C$ line widths of the filled polyisoprene obtained under magic-angle conditions are greater than the homogeneous line widths of the unfilled polymer, the average correlation frequency of the low-frequency interactions resulting from the influence of the filler, while small compared to the 22.6-MHz measuring frequency, must still be large compared to the 1-kHz spinning frequency. Thus, the broadened line can be only partially narrowed by magic-angle spinning.[3a]

**Acknowledgments.** The authors thank Dr. E. O. Stejskal (Monsanto Co., St. Louis, Mo.) and Dr. D. L. VanderHart (National Bureau of Standards, Washington, D. C.) for helpful discussions of the interpretations of the spinning and selective saturation experiments. The authors also thank Dr. J. Kim and Dr. V. Mochel (Firestone Tire and Rubber Co., Akron, Ohio) for the gift of the carbon-black-filled polyisoprene. S. H. C. and S. I. W. acknowledge the support of the National Institutes of Health.

# Electron Spin Resonance Studies of Frequencies of *Intra*molecular Collisions between the End Groups of a Hydrocarbon Chain

**H. D. Connor, K. Shimada, and M. Szwarc***

*SUNY Polymer Research Center, College of Forestry, Syracuse, New York 13210.* *Received June 12, 1972*

ABSTRACT: The frequency of *intra*molecular collisions between two groups linked to a polymer chain depends on chain flexibility, length of the polymer segment separating them, temperature, viscosity of the solvent, bulkiness of the attached groups, etc. We developed an esr technique which permits us to determine the frequency of such collisions and its dependence on the above parameters. This has been achieved by attaching two groups of relatively high electron affinity to the ends of the chain. Reduction of one of them to the respective radical anion yields a paramagnetic species characterized by its esr spectrum. Collision with the other end group results in electron transfer, and this affects the shape of the spectrum. A mathematical procedure has been described by means of which the frequency of collisions can be calculated from the shape of the experimental spectra. The results obtained at various temperatures for X–$(CH_2)_j$–X chains with $j$ equal to 3, 4, 5, 6, and 12 are reported.

Most polymeric molecules are flexible. This property arises from internal rotations around the covalent bonds of a polymeric chain that change its conformation. The flexibility of polymer chains endows these materials with their most valuable and useful properties. It makes many polymers plastic, provides elastic properties for rubbers, and permists many biopolymers to fulfill their vital biologic functions. Therefore, studies of the kinetics of conformational changes of polymer chains are important, and a novel approach to this problem is outlined in the present paper.

Consider a hydrocarbon chain, *e.g.*, one formed through linkage of $j$ $CH_2$ units and terminated by some groups X, *viz.*, X–$(CH_2)_j$–X. Continuous changes of conformation lead to collisions between the end groups, and the frequency of such *intra*molecular encounters depends on the flexibility of the chain, its length as determined by the value of $j$, temperature, viscosity of the solvent, bulkiness of the end groups, etc. A method of counting the frequency of such intramolecular collisions and its dependence on the above factors is therefore valuable in studies of kinetic problems associated with the chain's flexibility. The following technique led us to this goal.

Hydrocarbons having the general structure ($\alpha$-N)–$(CH_2)_j$–($\alpha$-N) with $j$ varying from 3 to 12 were synthesized,[1] $\alpha$-N

(1) P. Caluwe, K. Shimada, and M. Szwarc, *J. Amer. Chem. Soc.*, in press.

TABLE I
COUPLING CONSTANTS OF *n*-BUTYL-α-NAPHTHALENIDE[a]

| Proton | *a* in THF, G, at 10° | *a* in HMPA, G, at 25° | *a* in DME,[b] G |
|---|---|---|---|
| 2 | 1.60 | 1.53 | |
| 3 | 1.77 | 1.68 | |
| 4 | 4.10 | 4.46 | |
| 5 | 5.20 | 5.09 | |
| 6 | 1.65 | 1.62 | |
| 7 | 2.03 | 2.02 | |
| 8 | 5.10 | 4.89 | |
| 1′ | 2.58 | 2.78 | 2.80 |
| 2′ | 0.155 | 0.130 | −0.155 |
| 3′ | 0.045[b] | 0.045* | 0.045 |
| 4′ | 0.035[b] | 0.035* | 0.035 |

[a] Numbering as in structure I. The assignments are based on the analogy with the *a* constants reported for the radical anions α-methylnaphthalenide R. E. Moss, N. A. Ashford, R. G. Lawler, and G. K. Fraenkel, *J. Chem. Phys.*, **51**, 1765 (1969)] and α-ethylnaphthalenide (G. Moshuk, H. D. Connor, and M. Szwarc, *J. Phys. Chem.*, **76**, 1734 (1972). [b] E. de Boer and C. MacLean, *Mol. Phys.*, **7**, 191 (1965). The coupling constants for the 3′ and 4′ protons were assumed to be the same in THF and HMPA as those reported by de Boer for DME.

denoting an α-naphthyl group. These hydrocarbons were partially reduced with metallic potassium, and thus solutions of radical anions $(\alpha\text{-N}\cdot^-)\text{-}(CH_2)_j\text{-}(\alpha\text{-N})$ were prepared. The esr lines of these paramagnetic species are broadened by the intramolecular electron transfer

$$(\alpha\text{-N}\cdot^-)\text{-}(CH_2)_j\text{-}(\alpha\text{-N}) \longrightarrow (\alpha\text{-N})\text{-}(CH_2)_j\text{-}(\alpha\text{-N}\cdot^-)$$

and, provided that every collision is effective, the extent of the broadening measures the frequency of intramolecular collisions. (The investigated solutions were sufficiently dilute to make insignificant the contribution of *inter*molecular collisions to the electron-transfer process.) It is known[2] that electron transfers involving free-radical anions, but not ion pairs, are very fast; their rates are virtually diffusion controlled. Therefore, to obtain the required results we needed a solvent dissociating the ion pairs of $(\alpha\text{-N}\cdot^-)\text{-}(CH_2)_j\text{-}(\alpha\text{-N})$. The salts of aromatic radical anions are completely dissociated in hexamethylphosphortriamide[3] (HMPA), and therefore this solvent was chosen for our investigation. Similar studies involving $Ph\text{-}(CH_2)_j\text{-}Ph$ were attempted, but the behavior of the respective radical anions was unsatisfactory, preventing the contemplated study.

### Esr Spectrum of Radical Anions of α-Butylnaphthalene and the Rate of Intermolecular Exchange α-Bu-N·⁻ + α-Bu-N → Exchange

The evaluation of the results reported in the next section requires knowledge of the esr spectrum of some monofunctional model radical anion resembling $(\alpha\text{-N}\cdot^-)\text{-}(CH_2)_j\text{-}(\alpha\text{-N})$, *e.g.*, *n*-butyl-α-naphthalenide, α-Bu-N·⁻ (I), and of the rate of its *inter*molecular electron exchange with the parent hydrocarbon, α-Bu-N. The esr spectrum of α-Bu-N·⁻ should be identical with that of $(\alpha\text{-N}\cdot^-)\text{-}(CH_2)_j\text{-}(\alpha\text{-N})$ had the *intra*molecular electron transfer in the latter radical anion been

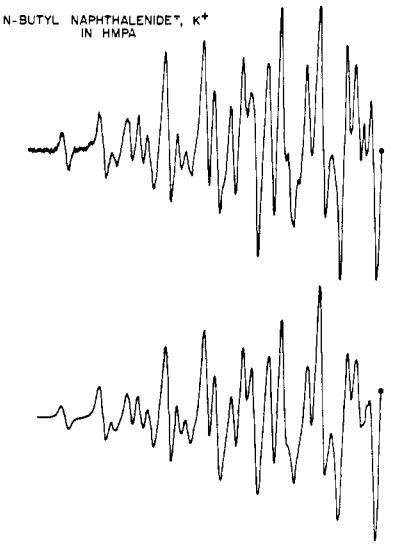


Figure 1. Esr spectrum of *n*-Bu-α-naphthalenide in HMPA at room temperature (only one half is displayed). (Below) The computer-simulated spectrum.

arrested. This expectation was verified by the subsequent results.

The esr spectra of the potassium salt of α-Bu-N·⁻ in tetrahydrofuran (THF) and in HMPA were examined. The spectrum obtained in the former solvent is sharp, and even the weak coupling to the 2′ protons is revealed by the partially

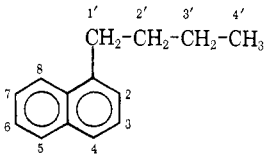


I

resolved triplet discerned in the extreme wing lines. The respective coupling constants were determined and are listed in Table I; their reliability was confirmed by computer simulation. The spectrum obtained from HMPA solution is less resolved (see Figure 1); however, its shape around its center has been found extremely sensitive even to minute changes in the values of the various coupling constants. Hence, in spite of the broadness of the spectrum, the coupling constants characterizing the radical anion in HMPA could be determined with a high degree of accuracy and the pertinent data are included in Table I. The computer-simulated spectrum based on these data is displayed in Figure 1 below the experimental spectrum, and inspection of this figure shows excellent agreement between both. By proper choice of the line width, we could also simulate the spectra of *n*-butyl-α-naphthalenide·⁻ observed in HMPA solution containing any desired concentration of the parent hydrocarbon (see, *e.g.*, Figure 3). Again, the agreement between the computed and observed spectra is excellent, provided the comparison is limited to the slow-exchange region.

The rate constant of the intermolecular electron transfer

$$\alpha\text{-Bu-N}\cdot^- + \alpha\text{-Bu-N} \longrightarrow \alpha\text{-Bu-N} + \alpha\text{-Bu-N}\cdot^-$$

in HMPA was determined in the limit of slow exchange by the method described by Weissman.[4] The increase in the width of the "first" line of the esr spectrum of α-Bu-N·⁻ was measured at various concentrations of the added α-Bu-N.

(2) (a) R. L. Ward and S. I. Weissman, *J. Amer. Chem. Soc.*, **79**, 2086 (1957); (b) P. J. Zandstra and S. I. Weissman, *ibid.*, **84**, 4408 (1962); (c) M. T. Jones and S. I. Weissman, *ibid.*, **84**, 4269 (1962); (d) N. Hirota, R. Carraway, and W. Schook, *ibid.*, **90**, 3611 (1968); (e) K. Höfelmann, J. Jagur-Grodzinski, and M. Szwarc, *ibid.*, **91**, 4645 (1969).

(3) A. Cserhegyi, J. Jagur-Grodzinski, and M. Szwarc, *ibid.*, 1892 (1969).

(4) Reference 2a.

The first line results from the overlap of three lines of a triplet with coupling constant 0.13 G (the interaction with the 2′ protons of the aliphatic chain) which are split further by the 3′ and 4′ protons (coupling constants 0.045 and 0.035 G, respectively). We obtained the computer-drawn lines of such multiplets for various line widths of the individual Lorentzian lines (300–900 mG), and measured the peak-to-peak distance of the resulting envelope. This permitted us to correct the observed line width, the resulting corrections being small for lines wider than 300 mG. A more significant correction is required to account for the overlap between the first and second lines of the spectrum. Such corrections again were introduced with the aid of computer-drawn spectra.

The final calculations led to the bimolecular rate constants for the intermolecular electron transfer listed in Table II. The Arrhenius plot, shown in Figure 2, is linear over the investigated temperature range and corresponds to the activation energy 4.8 kcal/mol and $A = 2.1 \times 10^{12}\ M^{-1}\ \text{sec}^{-1}$. The relatively high activation energy reflects the high activation energy of the diffusion process. The temperature dependence of the viscosity of HMPA was measured (the pertinent data are included in Table II), and the linear plot of $\log \eta$ *vs.* $1/T$ led to activation energy of 3.9 kcal/mol.

It is instructive to compare the observed rate constants with those calculated on the assumption of the diffusion-controlled reaction. Assuming that equal cross sections characterize the reaction and the diffusion process, the rate constant of the diffusion-controlled reaction is calculated to be $5.6 \times 10^{8}\ M^{-1}\ \text{sec}^{-1}$ at 30°. It is probable that the cross section for the electron transfer is greater than the Stokes cross section governing the rate of diffusion and, had this been the case, a more realistic constant for the diffusion-controlled rate might be even higher than quoted above. Comparison of these results with the experimentally obtained value suggests that virutally every encounter is effective in this electron-transfer process. (To be more precise, every second encounter would be effective, since there is equal probability for the electron to remain on the original N moiety as to be transferred to the other one.)

To strengthen this conclusion, we investigated the diffusion-controlled spin–spin exchange

$$\alpha\text{-Bu-N}\cdot^{-} + \alpha\text{-Bu-N}\cdot^{-} \longrightarrow \text{spin exchange}$$

The data, again derived from the broadening of the first line, are included in Table II and show that the spin–spin exchange and the electron-transfer proceed with similar rates. Hence, both processes appear to be diffusion controlled.

### The Esr Spectra of $(\alpha\text{-N}\cdot^{-})\text{-}(CH_2)_j\text{-}(\alpha\text{-N})$

At low rates of exchange the spectra of $(\alpha\text{-N}\cdot^{-})\text{-}(CH_2)_j\text{-}(\alpha\text{-N})$ should be identical with the esr spectra of *n*-butyl-α-naphthalenide recorded in a solution containing judiciously chosen concentration of *n*-butyl-α-naphthalene. This statement may appear questionable. In the *intra*molecular system exchanges in each pair occur between two naphthyl moieties having a fixed configuration of proton spins, the electron being alternately associated with one or the other partner of a pair. On the other hand, the transfer in the *inter*molecular system exchanges a naphthyl moiety having a particular configuration of proton spins into any other naphthyl moiety. Nevertheless, deeper consideration of the problem convincingly shows that this difference does not affect the shape of the esr spectrum provided the system is studied in the slow-exchange region. The relevant esr spectra become, however, different at the intermediate and fast exchange regions. In the limit of a fast exchange the spectrum of the (α-naphthalenide·⁻)-$(CH_2)_j$-(α-naphthyl) becomes indistinguishable from that of a hypothetical "dimer," (α-*n*-butylnaphthalene)$_2\cdot^{-}$, whereas the esr spectrum of α-*n*-butylnaphthalenide·⁻ mixed with α-*n*-butylnaphthalene loses its hyperfine structure and appears then as a broad structureless line.

The pertinent esr spectra are seen in Figures 3–8. Figure 3 shows the spectra of $\alpha\text{-Bu-N}\cdot^{-}$ in $2.7 \times 10^{-2}\ M$ HMPA solution of α-Bu-N recorded at temperatures varying from −15 to 45°. (It is possible to supercool HMPA to −15° without freezing the solution.) At this concentration of α-Bu-N the spectrum of $\alpha\text{-BuN}\cdot^{-}$ observed at −15° is identical with the spectrum of $(\alpha\text{-N}\cdot^{-})\text{-}(CH_2)_{12}\text{-}(\alpha\text{-N})$ recorded at the same temperature (see the lowest spectrum in Figure 4). Hence, at −15°, the rate of the *intra*molecular collisions for $j = 12$ is the same as the rate of the bimolecular collisions $\alpha\text{-Bu-N}\cdot^{-} + \alpha\text{-Bu-N}$ at $2.7 \times 10^{-2}\ M$ concentration of α-*n*-butylnaphthalene.

TABLE II
RATE CONSTANTS FOR ELECTRON TRANSFER IN HMPA, $n\text{-Bu-}\alpha\text{-N}\cdot^{-} + n\text{-Bu-}\alpha\text{-N} \rightarrow n\text{-Bu-}\alpha\text{-N} + n\text{-Bu-}\alpha\text{-N}\cdot^{-}$, FOR THE RELEVANT SPIN–SPIN EXCHANGE, AND FOR HMPA VISCOSITY

| Temp, °C | $k$(electron transfer), $M^{-1}\ \text{sec}^{-1}$ [a,c] | $k$(spin exchange), $M^{-1}\ \text{sec}^{-1}$ [a,b] | $\eta$, cP, HMPA |
|---|---|---|---|
| −15 | $1.9 \times 10^{8}$ | $3.4 \times 10^{8}$ | |
| 0 | $3.5 \times 10^{8}$ | $5.6 \times 10^{8}$ | 6.23 |
| 15 | $6.1 \times 10^{8}$ | $7.6 \times 10^{8}$ | 4.24 |
| 30 | $9.1 \times 10^{8}$ | $9.0 \times 10^{8}$ | 3.03 |
| 45 | $11.6 \times 10^{8}$ | $14.5 \times 10^{8}$ | 2.22 |
| 60 | | | 1.71 |

$E$(electron transfer) = 4.8 kcal/mol
$E$(spin exchange) = 3.6 kcal/mol
$-E$(viscosity) = 3.9 kcal/mol

[a] The rate constants were determined from the concentration dependence of the line width of the end line of the esr spectra. The values for the line width were corrected for the effects of overlap from the next line. [b] The spin-exchange studies were done by varying the radical concentrations from $2.63 \times 10^{-3}$ to $16.1 \times 10^{-3}\ M$. [c] $[n\text{-BuN}\cdot^{-}] = 8 \times 10^{-4}\ M$.

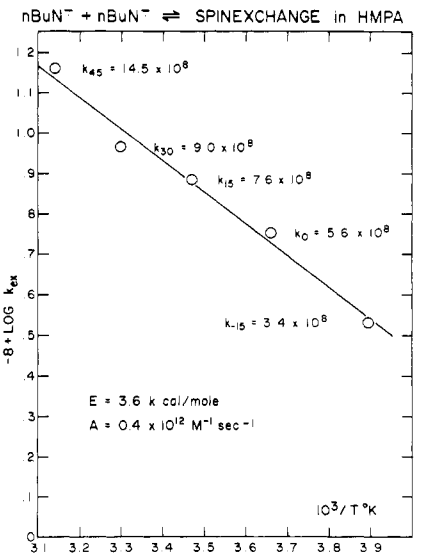


Figure 2. Arrhenius plot of the bimolecular rate constants of the spin–spin exchange $n\text{-Bu-}\alpha\text{-N}\cdot^{-} + n\text{-Bu-}\alpha\text{-N}$. A similar plot was obtained for the electron-transfer process.

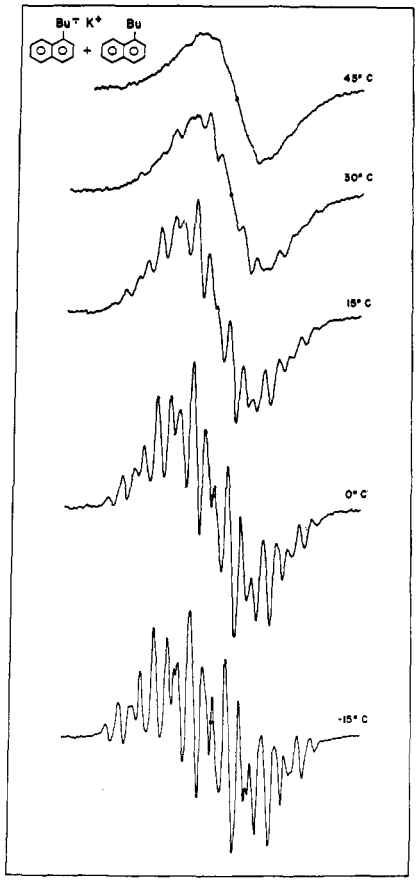

Figure 3. Esr spectra of *n*-Bu-α-N·⁻. in 2.7 × $10^{-2}$ *M* solution of *n*-Bu-α-N in HMPA recorded at −15, 0, 15, 30, and 45°.

The rate of collisions increases as the temperature rises, and subsequently the esr spectra of the *inter*- and *intra*molecular systems become broader at higher temperatures. However, their shapes are now different. A new pattern of lines seems to develop at 45° in the spectrum of the *intra*molecular system (see Figure 4), whereas the hyperfine structure is lost in the spectrum of the *inter*molecular system at that temperature (see Figure 3).

It has not been feasible to increase further the rate of collisions by increasing temperature, since a decomposition of the radical anions takes place above 45°. But the rate of *intra*molecular transfer could be increased by reducing the length of the chain connecting the naphthyl moieties. Indeed, inspection of Figure 5 shows that the rate of the *intra*molecular collisions of (α-N·⁻)-$(CH_2)_4$-(α-N) ($j$ = 4) at −15° is comparable to that observed for the radical with $j$ = 12 at 45°, the respective two spectra being remarkably similar (compare Figures 4 and 5). As the temperature of the solution of (α-N·⁻)-$(CH_2)_4$-(α-N) rises, the increase in the rate leads now to sharpening, and not broadening, of the lines, and at 45° the spectrum of a new species is clearly discerned.

For $j$ = 3 the rate of collisions is very fast and, not surprisingly, the pertinent spectra are those of the new species (see Figure 6); even at −15° the new pattern of lines is sharp. On the other hand, the spectra of radical ions derived from hydrocarbons with $j$ = 5 (Figure 7) and $j$ = 6 (Figure 8) reveal the transition from a slow to a fast exchange region, verifying the lower rate for higher $j$.

Let us demonstrate that the esr spectra shown in Figures 5 and 6 are those of the hypothetical dimer, $(-CH_2-\alpha\text{-N})_2\cdot^-$. An electron associated with such a dimer interacts with twice

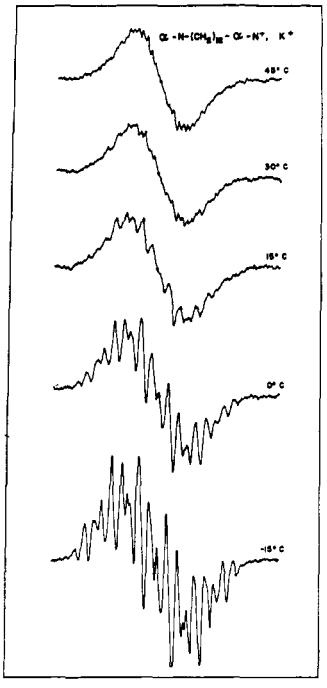

Figure 4. Esr spectra of (α-N·⁻)-$(CH_2)_{12}$-(α-N) in HMPA recorded at −15, 0, 15, 30, and 45°.

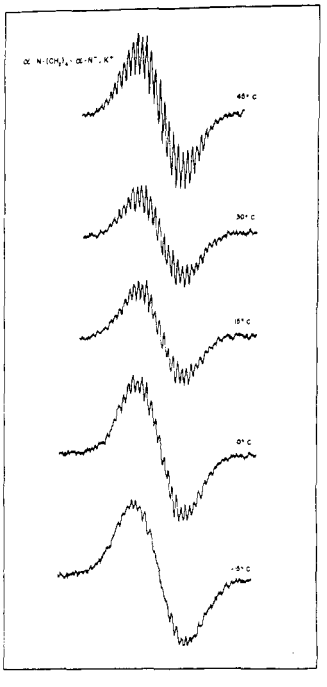

Figure 5. Esr spectra of (α-N·⁻)-$(CH_2)_4$-(α-N) in HMPA recorded at −15, 0, 15, 30, and 45°.

as many protons as an electron located on *n*-butyl-α-naphthalene, but in the former species the coupling constants should be one-half of those found for the corresponding protons of the latter radical anion. Reliable values of the coupling constants for *n*-butyl-α-naphthalenide are given in Table I, and hence a computer-simulated spectrum of the dimer could be drawn. Such a spectrum, shown in Figure 9, is identical with the spectrum of (α-N·⁻)-$(CH_2)_3$-(α-N) displayed in the same figure below the computed spectrum. Thus, it is proved that the spectra of (α-N·⁻)-$(CH_2)_j$-(α-N) approach that of the dimer in the limit of fast exchange.

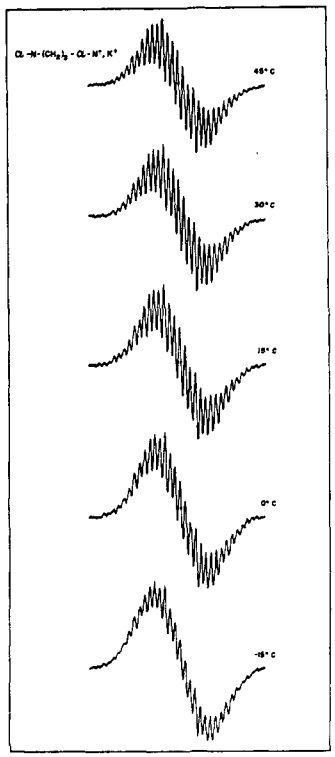

Figure 6. Esr spectra of (α-N·⁻)-$(CH_2)_3$-(α-N) recorded at −15, 0, 15, 30, and 45°.

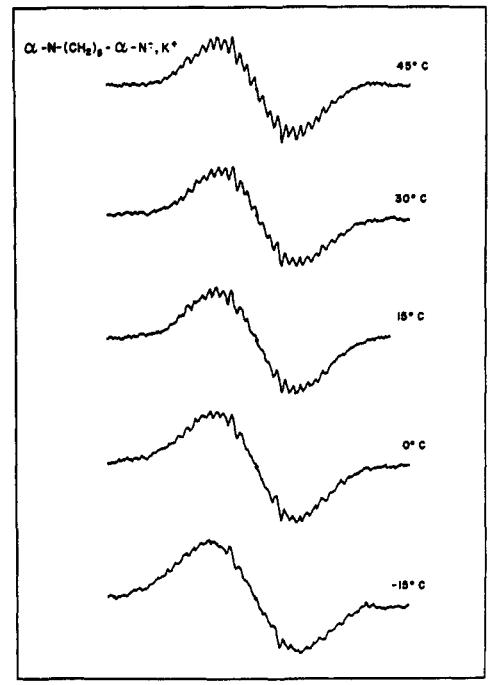

Figure 7. Esr spectra of (α-N·⁻)-$(CH_2)_5$-(α-N) in HMPA recorded at −15, 0, 15, 30, and 45°.

### Calculation of the Esr Spectra of the Exchanging System

Our starting point is the solution of the Bloch equation for the absorption line arising from the electron exchange in a hypothetical molecule containing two sites of different electron-spin transition energies. The derivation based on the standard expression[5] gives the complex magnetization, $\hat{M}$, equal to

$$\hat{M} = \gamma_e H_1 M_0 \times \frac{\omega - \bar{\omega} + i/T_2 + 2iP}{(\omega - \omega_A + i/T_2)(\omega - \omega_B + i/T_2) + 2iP(\omega - \bar{\omega} + i/T_2)}$$

where $\omega_A$ and $\omega_B$ are the resonance frequencies of the transition at the two sites, $\bar{\omega}$ is $\frac{1}{2}(\omega_A + \omega_B)$, and $P$ is the frequency of jumping. The imaginary part of $\hat{M}$ gives the intensity of the esr absorption, $v$, at frequency $\omega$, *i.e.*,

$$v = \gamma_e H_1 M_0 \left\{ \frac{1}{2} P(\omega_A - \omega_B)^2 + 2(\omega - \bar{\omega})^2/T_2 - (\omega - \omega_A)(\omega - \omega_B)/T_2 + 4P^2/T_2 + 4P/T_2^2 + 1/T_2^3 \right\} \Big/ \left\{ [(\omega - \omega_A)(\omega - \omega_B) - 2P/T_2 - 1/T_2^2]^2 + 4(\omega - \bar{\omega})^2(1/T_2 + P)^2 \right\}$$

Calculation of the esr spectrum of (α-N·⁻)-$(CH_2)_f$-(α-N) requires the addition of the $v$ terms involving all possible pairs of proton spin configurations of the two exchanging naphthyl moieties. Owing to the limitation on computer time it was not possible to consider the 2′, 3′, etc. protons in the total spin configuration. Their coupling constants are small and unresolved in the hyperfine structure resulting from the remaining protons. Hence, the 384 line spectrum

(5) A. Carrington and A. D. McLachlan, "Introduction to Magnetic Resonance," Harper and Row, New York, N. Y., 1967, pp 205–207.

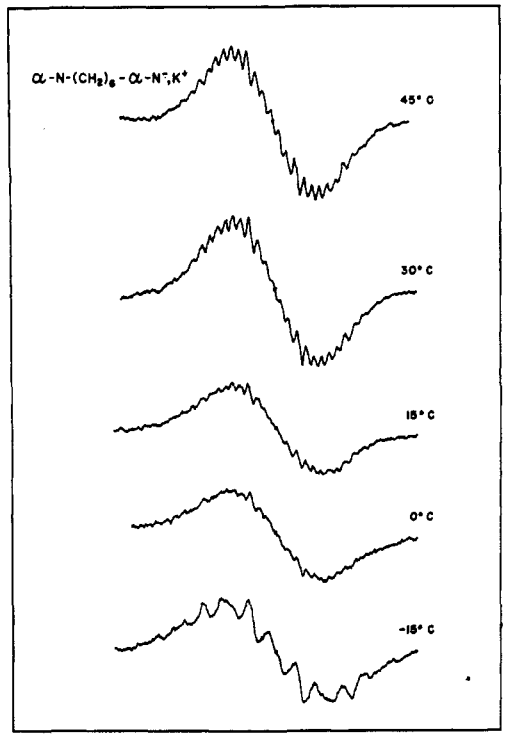

Figure 8. Esr spectra of (α-N·⁻)-$(CH_2)_6$-(α-N) in HMPA recorded at −15, 0, 15, 30, and 45°.

of the -$CH_2$-(α-N) moiety consists of lines broader than would be expected on the basis of the usual $T_2$ of this type of system. This necessitated the use of a larger value for the effective $1/T_2$ in the equation giving $v$.

The value of the required effective $1/T_2$ was obtained by computer simulation of a single line resulting from the overlap of the unresolved lines at different values of $P$. Such lines were computed by the method outlined above for three pairs of protons with coupling constants of 0.130, 0.045, and 0.035

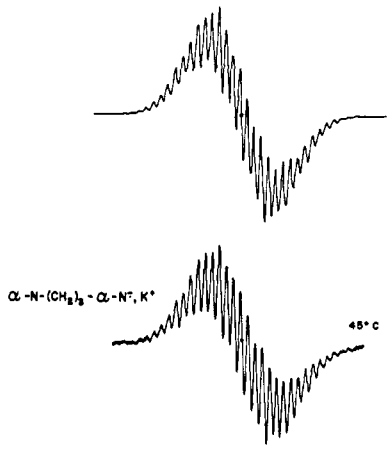


Figure 9. Computer-simulated esr spectrum of the hypothetical dimer $(-CH_2-\alpha\text{-}N)_2\cdot^-$ (coupling constant being one-half of those given in Table I). (Below) The esr spectrum of $(\alpha\text{-}N\cdot^-)$-$(CH_2)_8$-$(\alpha\text{-}N)$ in HMPA at 30°.

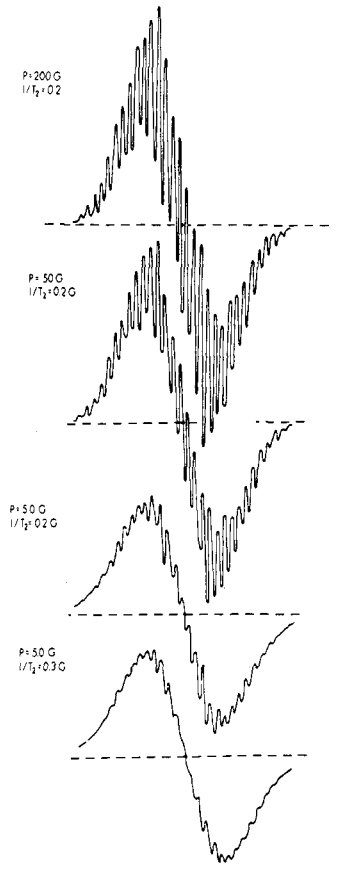


Figure 10. Calculated esr spectra of the exchanging $(\alpha\text{-}N\cdot^-)$-$(CH_2)_j$-$(\alpha\text{-}N)$ radical anions computed for various frequencies, $P$, of electron transfer.

G, respectively (see Table I), assuming $1/T_2 = 0.01$ G and $P = 1$, 5, 50, and 500 G, The resulting lines are virtually Lorentzian, and all correspond to an apparent $1/T_2$ of 0.2 G. Therefore, this value of $1/T_2$ was used in our calculations.

The esr spectrum of an exchanging radical anion, $(\alpha\text{-}N\cdot^-)$-$(CH_2)_j$-$(\alpha\text{-}N)$, is then calculated by adding the $v$ terms for $(512)^2$ pairs corresponding to all the lines resulting from the electron coupling to seven aromatic and two aliphatic ($C^{1\prime}$) protons. To avoid the weighting factors in the summation, the latter two protons were counted as distinct although having the same coupling constant. This procedure gives the absorption spectrum, and its differentiation produces the conventional esr spectrum.

The spectra calculated for $P = 200$, 50, and 5 G, respectively, with $1/T_2 = 0.2$ G are shown in Figure 10. As expected, they are identical with those of the dimer, but each looks as if it corresponds to a different value of line width of the individual lines. Hence, we are now in a position to associate the shape of each spectrum to a definite frequency of *intra*molecular collisions. The relation with $P$ is reflected, *e.g.*, in a relative height of the teeth compared with the height of the whole spectrum. This ratio provides a sensitive parameter for calculating $P$.

The spectrum computed for $P = 0.3$ G resembles the one obtained at slow rate of exchange, *e.g.*, that shown in Figure 4 at 0°.

### Frequency of Intramolecular Collisions

The data presented in the previous sections permit us to calculate and discuss the frequency of *intra*molecular collisions. As demonstrated by the esr spectra shown in Figures 3 and 4, the rate of such collisions in the $(\alpha\text{-}N\cdot^-)$-$(CH_2)_{12}$-$(\alpha\text{-}N)$ system at $-15°$ was found to be approximately the same as the rate of *inter*molecular collisions, $\alpha$-Bu-N$\cdot^-$ + $\alpha$-Bu-N, proceeding at the same temperature and at the concentration of $\alpha$-Bu-N of $2.7 \times 10^{-2}$ $M$. The bimolecular rate constant determined at $-15°$ is $2 \times 10^8$ $M^{-1}$ sec$^{-1}$, hence the frequency of the *intra*molecular collisions in the $j = 12$ system is about $10^7$ sec$^{-1}$ at that temperature (twice the rate of transfer).

The *intra*molecular collisions may be treated as if they were *inter*molecular collisions at the electron acceptor "concentration" equivalent to one molecule per sphere of a radius equal to the length of the extended chain. Surely, this is the *lower* limit for the more realistic concentration which should be still higher, because the acceptor molecule is rarely found close to the surface of the sphere—such an event requires the improbable full extension of the chain. On this basis we calculate the concentration of naphthyl moieties for the system $C_{12}$ to be at least 0.07 $M$. However, as shown previously, the *intra*molecular collisions proceed in this system with the same rate as the *inter*molecular process at the concentration of the acceptor, *i.e.*, $\alpha$-Bu-N, of only $2.7 \times 10^{-2}$ $M$. Hence, the *inter*molecular process seems to be about 3 times faster than the equivalent *intra*molecular transfer. The *intra*molecular collisions require cooperative rotation of the various C–C bonds in addition to the motion of $\alpha$-N moieties, and apparently the hindrance encountered in such rotations is responsible for its relative slowness when compared with the *inter*molecular one.

### Electron Transfer Resulting from Transfer through an Alkyl Chain

Several investigators[6-10] considered electron transfer between two identical aromatic moieties linked by a chain. Their treatment assumed some weak coupling interaction between both aromatic groups, leading to lifting of the degeneracy and subsequently to the *intra*molecular resonance charge transfer. Any perturbation reducing the symmetry of the system, caused, *e.g.*, by the polarization of solvent

(6) S. I. Weissman, *J. Amer. Chem. Soc.*, **80**, 6462 (1958).
(7) V. V. Voevodskii, S. P. Solodovnikov, and V. M. Chibrikin, *Dokl. Akad. Nauk* SSSR, **129**, 1082 (1959).
(8) H. M. McConnell, *J. Chem. Phys.*, **33**, 508 (1961).
(9) J. E. Harriman and A. Maki, *ibid.*, **39**, 778 (1963).
(10) F. Gerson and W. B. Martin, Jr., *J. Amer. Chem. Soc.*, **91**, 1883 (1969).

molecules around the moiety bearing the charge, results in trapping of the electron on one or the other aromatic group. The calculation by Harriman and Maki[9] showed that such a perturbation results in the frequency of transfer greater than $10^8$ sec$^{-1}$ when the relevant groups are linked by one $CH_2$ unit; however, it decreases to about $10^6$ sec$^{-1}$, or less, when the linking bridge consists of a chain of two carbons, *i.e.*, $(CH_2)_2$. Similar calculations by McConnel[8] show that insertion of each additional $CH_2$ unit to the linking bridge reduces the frequency of the transfer by at least a power of ten.

Our experimental results yield the frequency of transfer due to the *intra*molecular collisions of about $10^8$–$10^9$ sec$^{-1}$ for the ($\alpha$-N$\cdot^-$)-$(CH_2)_3$-($\alpha$-N) system. Hence, the contribution of the direct through-chain transfer to the process observed by us is negligible. Such a contribution, if any, is even less important for $j > 3$.

Let us remark that for $j = 2$ the *intra*molecular collisions are impossible due to steric constraint. In such systems, therefore, the electron transfer may result only from causes discussed above.

In conclusion, it has been shown that a method is available for determining the rate of *intra*molecular collisions between the ends of a polymeric chain, as well as its dependence on the chain's length, temperature, etc. The dependence on the chain's length is particularly interesting for short chains, since the restrictions arising from unfavorable conformations are less understood in such systems than in those involving long chains. The final results of such calculations and their discussion will be published later.

Obviously, much additional work is needed. The effect of large end groups, acting as dampers, should be investigated. Therefore, we intend to study the behavior of chains terminated by smaller as well as by bigger groups. Further extension of these studies calls for the investigation of collisions between end groups linked by other chains as well as collisions in solvents of different viscosity.

**Acknowledgment.** The financial support of these studies by the National Science Foundation is gratefully acknowledged.

# Two-Stage Synthesis of Poly(*N*-phenylbenzimidazoles)

**V. V. Korshak, A. L. Rusanov,* D. S. Tugushi, and G. M. Cherkasova***

*Institute of Elementorganic Compounds, Academy of Sciences of the USSR, Moscow, USSR.* *Received April 12, 1972*

ABSTRACT: The low-temperature solution condensation of either 1,3-dianilino-4,6-diaminobenzene, 3,3′-diamino-4,4′-dianilinodiphenyl, or 3,3′-diamino-4,4′-dianilinodiphenyl sulfone in combination with various dicarboxylic acid dichlorides leads to high molecular weight poly(*o*-phenylaminoamides). The solid-state polycyclodehydration of poly(*o*-phenylaminoamides) leads to poly(*N*-phenylbenzimidazoles) soluble in organic solvents. The effect of polymer structure on solubility, glass transition, and decomposition temperatures was investigated.

The synthesis of poly(*N*-phenylbenzimidazoles) by melt polycondensation of bis(*N*-phenyl-*o*-phenylenediamines) with dicarboxylic acid diphenyl esters has been reported by several investigators.[1,2] Poly(*N*-phenylbenzimidazoles) exhibit good solubility and thermooxidative stability, but their molecular weights are relatively low. In this investigation we used the two-stage process to synthesize high molecular weight poly(*N*-phenylbenzimidazoles).

## Discussion

**Model Compounds.** Prior to polymer synthesis, a series of model compounds shown in Table I was prepared to obtain information on the conditions of polymer formation and to identify them.[3] The model compounds were prepared by the reaction of benzoyl chloride with *o*-aminodiphenylamine and also with various bis(*N*-phenyl-*o*-phenylenediamines) and by the reaction of *o*-aminodiphenylamine with various aromatic dicarboxylic acid chlorides (eq 1–3).

The intermediates, *N*-phenyl-*N*′-aroylene-*o*-phenylenediamines, were prepared by low-temperature solution condensation in *N*,*N*-dimethylacetamide or *N*-methyl-2-pyrrolidone in quantitative yields. The conversion to 1,2-diphenylbenzimidazoles was effected at elevated temperatures in solid state or in the melt.

The infrared spectra of some model compounds are shown in Figures 1 and 2; the ultraviolet spectral data for the model compounds are given in Table I. In accordance with the dta and tga data, all model compounds degrade in two stages; degradation begins in the temperature range from 340 to 370° and is accompanied by partial sublimation of products.

**Polymers.** The polymers were synthesized by the reaction of bis(*N*-phenyl-*o*-phenylenediamines) with dicarboxylic acid chlorides followed by cyclization of the resulting poly(*o*-phenylaminoamides) as shown on p 809, column 2 at bottom.

The high molecular weight polymer precursors ($\eta_{red}$ = 0.2–2.5), poly(*o*-phenylaminoamides), were prepared by low-temperature polycondensation (0–20°) in *N*,*N*-dimethylacetamide or *N*-methyl-2-pyrrolidone. In contrast with unsubstituted bis(*o*-phenylenediamines), the tetramines used in these reactions behave as bifunctional monomers because of the great difference in the nucleophilic reactivities of amino and imino groups doubly joined in positions ortho to each other;[4] as a result it is possible to add the solid dicarboxylic

(1) H. Vogel and C. S. Marvel, *J. Polym. Sci., Part A*, **1**, 1531 (1963).
(2) V. V. Korshak, G. M. Tseitlin, G. M. Cherkasova, A. L. Rusanov, and N. A. Berezkina, *Vysokomol. Soedin. A*, **11**, 35 (1969).
(3) V. V. Korshak, A. L. Rusanov, D. S. Tugushi, and S. N. Leontjeva, *Chim. Heterocycl. Soedin.*, in press.
(4) V. V. Korshak and A. L. Rusanov, *Izv. Akad. Nauk SSSR, Ser. Khim.*, 289 (1970); *Polimery(Poland)*, **15**, 400 (1970).